applied sciences

MDPI

Article

Development of High-Power Ultrasonic System Dedicated to Metal Powder Atomization

Pawel Kustron, Marcin Korzeniowski, Adam Sajbura, Tomasz Piwowarczyk, Pawel Kaczynski and Pawel Sokolowski *

Faculty of Mechanical Engineering, Wroclaw University of Science and Technology, Lukasiewicza 5, 50-371 Wroclaw, Poland; pawel.kustron@pwr.edu.pl (P.K.); marcin.korzeniowski@pwr.edu.pl (M.K.); adam.sajbura@pwr.edu.pl (A.S.); tomasz.piwowarczyk@pwr.edu.pl (T.P.); pawel.kaczynski@pwr.edu.pl (P.K.)
* Correspondence: pawel.sokolowski@pwr.edu.pl; Tel.: +48-71-320-2148

Featured Application: The presented work considers the ultrasonic atomization as a novel approach for metal and metal alloy powder manufacturing.

Abstract: The article presents the results of the development works and research on the atomization process carried out using two prototype high-power ultrasonic systems. Ultrasonic systems have been designed to develop a new metal powder production process; these materials are increasingly used in modern manufacturing processes such as additive technologies or spraying and surfacing processes. The preliminary studies presented in the article were conducted for water to assess the effectiveness of both systems and to verify the theoretical and structural assumptions. In ultrasonic atomization, the ultrasonic wave causes the phenomenon of cavitation, which leads to the overcoming of the surface tension forces of the liquid and its disintegration into fine droplets. The important parameters that affect the properties of the produced droplets include, among others, the frequency of the sonotrode vibrations and the amplitude of the vibrations of the working plate. As part of the research, the paper presents the process of selecting the sonotrode geometry for two different values of the transducer's natural frequencies (20 kHz and 70 kHz). In the design process, the finite element method was used to perform a harmonic analysis and develop the geometry of the sonotrode and the working plate. The design assumptions and the design process were presented. The modeled and then ultrasonic waveguides were verified experimentally by measuring the deflection distribution on the working plate surface using a high-precision laser displacement sensor. Then, the work ultimately resulted in conducting atomization tests of water. The obtained aerosols and the mechanism of their formation were studied using a high-speed camera. Finally, using Matlab R2020a software and image analysis scripts, it was possible to analyze the droplet size distribution generated by both systems. It was observed that 50% of the produced droplets were in the range of 35–55 µm for a 20 kHz system, while for a 70 kHz system it was 10–25 µm, which is a very satisfying distribution in terms of metal powder atomization.

Keywords: ultrasound; atomization; ultrasonic atomization; metal powder; sonotrode

check for updates

Citation: Kustron, P.; Korzeniowski, M.; Sajbura, A.; Piwowarczyk, T.; Kaczynski, P.; Sokolowski, P. Development of High-Power Ultrasonic System Dedicated to Metal Powder Atomization. *Appl. Sci.* **2023**, *13*, 8984. https://doi.org/10.3390/app13158984

Academic Editor: Giuseppe Lacidogna

Received: 30 June 2023
Revised: 28 July 2023
Accepted: 30 July 2023
Published: 5 August 2023

1. Introduction

Ultrasonic (UT) atomization is a phenomenon involving the disintegration of droplets or a stream of liquid and the formation of an aerosol under the influence of ultrasonic waves, including high-power ones. Ultrasonic atomization, like other atomization methods, uses the energy supplied by an external medium to disintegrate a liquid as a result of bringing it out of a stable state [1]. In this characteristic atomization method, energy is carried by ultrasonic waves, which cause an increase in pressure in the droplets of liquid located on the surface of the sonotrode [2]. When the critical value is exceeded, the liquid breaks down into very fine droplets. Ultrasonic atomization has found its application in medicine as a method of administering inhaled drugs (inhalation support) and the production of medicines and chemistry—for the separation of fractions with different properties and mechanics—for example for the production of protective coatings [2–4]. It should be emphasized that the phenomenon of ultrasonic atomization of liquids is well understood. However, its practical application is limited to typical liquids such as aqueous solutions, alcohols or fats.

Recently, ultrasonic atomizers have also been considered as a novel approach for metal and metal alloy powder production. The idea assumes that the ultrasonic vibrations are used to disintegrate the molten metal and create fine metal or metal alloy droplets, which later, after the solidification, form fine and spherical powder particles. Such materials are usually produced by other atomization processes, with gas, water and plasma atomization considered as state-of-art technologies. Ultrasonic atomization cannot replace typical industrial, large-volume atomization processes, but can be an interesting alternative in the case of the development, laboratory-scale or on-demand production, especially of rare or high-quality powder materials. Ultrasonically induced atomization process has a few significant advantages, mainly stable and predictable dependences between the operating parameters and vibration characteristics, atomization rate or droplet diameter [5,6]. Furthermore, UT atomization is known to produce very narrow droplet size distribution, so this may allow producing powders tailored for specific manufacturing processes and limit the material losses. In terms of metal powder production, it is also important that the process can be operated in a small chamber, consuming much less energy, gas or other media when compared to other atomization methods. It was demonstrated in the literature that the ultrasonic atomization was already laboratory-tested for the production of various advanced metal alloys or even composite materials, including: aluminum matrix composites (AMCs) [7]; Zr-based metallic glass [8]; refractory Mo-Si-Ti alloys [9]; stainless steel [10,11]; lightweight and low-melting-point alloys, like Al-Cu- [12], Al-Si- [13] or Bi-based alloys [14].

This work presents the first stage of the ultrasonic atomization technology development, dedicated to metal powder production. The designing and experimental verification of two high-power ultrasonic set-ups, operating at 20 kHz and 70 kHz, are shown here. The UT atomization capabilities of both set-ups were measured by a precise displacement sensor and then observed with a high-speed camera when the disks were loaded with water. The distribution of atomized water droplets, depending on the operating frequency, was also analyzed. The ultrasonic waveguides were designed to have atomizing disks with the diameters of 140 mm, so they can effectively work later with different melting set-ups and the atomization may be done effectively over a large surface. Up to the knowledge of authors, such UT systems were not tested yet in the context of metal powder production.

2. Ultrasonic Atomization Phenomena

The physical mechanism of the phenomenon that causes the atomization effect is broadly studied by many scientific centers and described through various mathematical models [15]. According to one of the hypotheses presented by Lierke [16], the phenomenon of atomization of liquid metals occurs as a result of the formation of surface waves in the liquid metal layer. A large amplitude of vibration overcomes the surface tension forces and detaches the droplets (Figure 1).

In many publications, e.g., [11,17–19], ultrasonic atomization of various liquids is described as an effect of cavitation phenomenon. High-power vibrations cause creation of the so-called cavitation bubbles. They break the surface tension of the liquid, allowing its atomization when it comes in contact with the surface of the sonotrode's working (vibrating) element [11,17–19]. Depending on the process parameters, with the operating frequency as one of the most important one (see Figure 1), but also the kind of a liquid, it is possible to obtain droplets of various sizes and shapes. In the case of metal powder materials, the aim is to obtain powders with a spheroidal geometry and a narrow particle size distribution. This is the most influenced by two parameters of the ultrasonic system, i.e., the frequency and amplitude of the working tool vibrations. In addition, in this case, the physical properties of the liquid metal, such as viscosity, surface tension, temperature and others, are important [18].

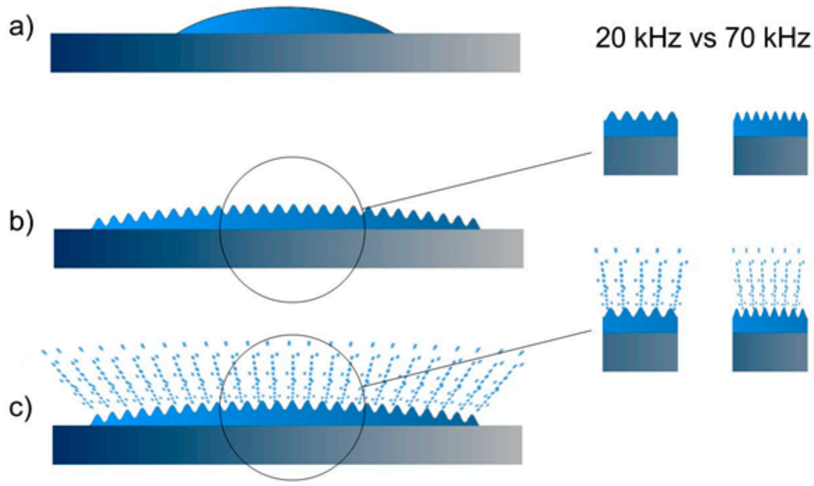

Figure 1. Diagram of the phenomenon of atomization of liquids: (**a**) a droplet on the surface of the plate, (**b**) formation of the capillary waves depending e.g., on the operating frequency, and (**c**) the appearance of liquid droplets in the atomization process (where the higher frequency should cause the release of finer droplets).

According to the literature [17], the amplitude of vibrations should exceed a certain threshold value to initiate the atomization process. This level can be calculated using Equation (1) [17]

$$A_m = \frac{2\mu}{\rho} \sqrt[3]{\frac{\rho}{\pi\sigma f}} \,, \tag{1}$$

where: A_m—threshold value of the amplitude [µm], μ—dynamic viscosity [Pa*s], ρ—liquid density [kg/m^3], σ—surface tension [N/m] and f—vibrations frequency [Hz].

On the ultrasonic system side, the vibration amplitude of the ultrasonic transducer can be adjusted by converting the excitation voltage value [17,19,20]. In addition, according to the assumptions of the surface wave model, increasing the frequency of the transducer's vibrations results in the formation of smaller droplets. This phenomenon is described by Equation (2) [11,17]

$$d = 0.34 \sqrt[3]{\frac{8\pi\sigma}{\rho f^2}} \,, \tag{2}$$

where: d—droplets diameter [µm], σ—surface tension [N/m], ρ—metal density [kg/m^3] and f—vibrations frequency [Hz].

It can be found in the literature that the increase in the temperature of a liquid metal causes a decrease in particle size due to e.g., reduction of its surface tension [19]. In addition, the atomization process of liquid metals can be carried out in a protective atmosphere of argon, nitrogen or in the vacuum, which leads to the formation of spheroidal particles. The small presence of oxygen during the process usually leads to deviations of the particle geometry from the nodular shape [18,19].

Taking into account the above equations and literature data on material properties, it is possible to analytically determine the amplitude threshold values and droplet diameters for the two selected media, i.e., liquid metal and water. The material data, as well as the calculated values, are presented in Table 1 [21].

Table 1. Material properties [21] and calculated values of amplitude threshold and droplet diameter.

Medium	Density ρ [kg/m^3]	Surface Tension σ [N/m]	Dynamic Viscosity μ [mPa*s]	A_m (Frequency 20 kHz) [µm]	d (Frequency 20 kHz) [µm]	A_m (Frequency 70 kHz) [µm]	d (Frequency 70 kHz) [µm]
Water	1000	0.07	1.0016	1.223	55.70	0.805	24.16
Liquid metal	7220	1.872	5.443	0.595	86.15	0.392	37.37

3. Materials and Methods

3.1. Ultrasonic Atomization Set-Up Idea

The target atomization system consists of: melting system and ultrasonic system closed in a working chamber but also control system, ultrasonic generator, cooling systems, diagnostics, etc. However, the design phase began with two key components, i.e., the melting system and the ultrasonic atomization system. The idea of combining both components was presented schematically in Figure 2.

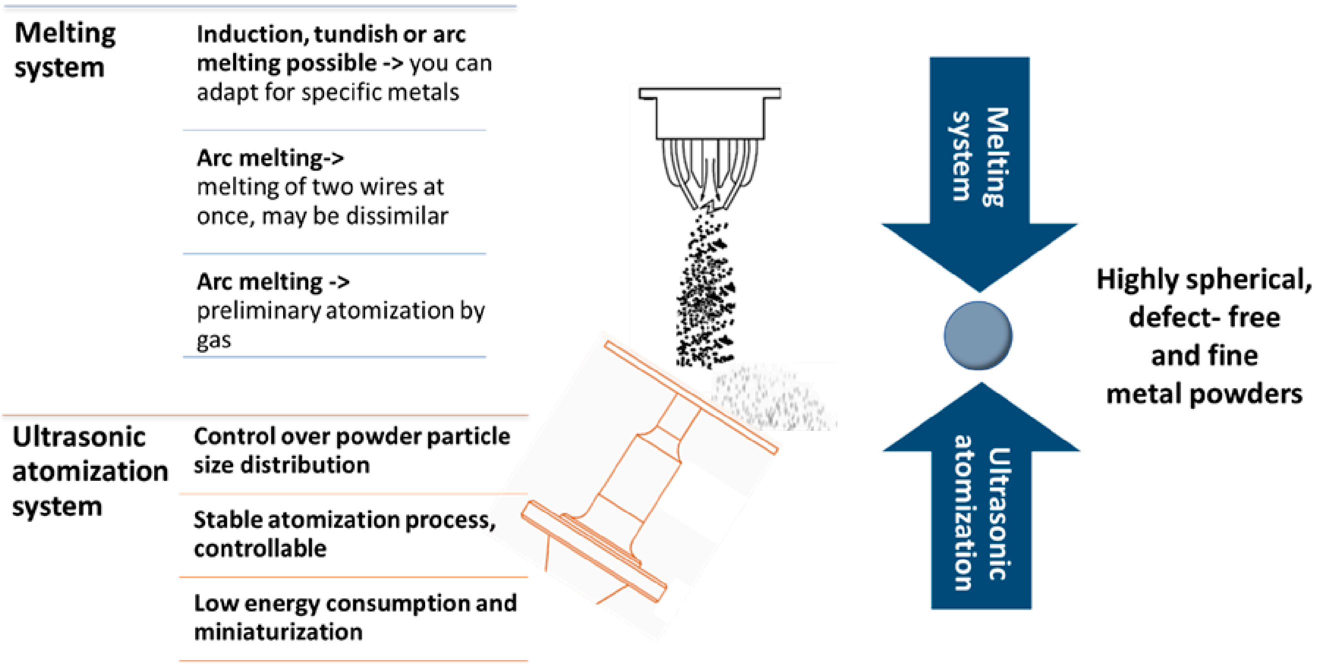

Figure 2. The idea of an ultrasonic atomization set-up for metal powders production.

The most important part and the 'hearth' of the ultrasonic atomization system was the ultrasonic waveguide. Two UT systems working with different frequencies were assumed here, 20 kHz and 70 kHz, due to the significant impact of this parameter on the size of the resulting droplet of atomized metal [15], which was also discussed in the previous chapter. In addition, it should be noted that with an increase in frequency, it is more difficult to achieve a high amplitude of vibrations and an even distribution of amplitude on the surface of the working plate. For this reason, 70 kHz was adopted as the maximum frequency. The design process took into account the mechanical characteristics of the sonotrode materials, considering its shape-dimensional relationships and possible temperature changes during the process (temperature increase induced by the molten metal). As a power transducer, the use of a Langevin type transducer is assumed to obtain the required amplitude of vibrations on the surface of the sonotrode's working plate.

The second parameter was the size of the vibrating plate, which is supposed to have direct contact with the stream of the molten metal. The Twin-Wire Arc Spraying (TWAS) process was considered here as a method of melting the wire feedstock materials by an electric arc. The melting process has mainly been studied in terms of controlling the geometry and direction of the liquid material stream, based on the preselection of TWAS process parameters, i.e., working gas pressure [bar], wire feed speed [m/min], intensity [A] and arc voltage [V], and others. The melting process was also investigated and verified in terms of in-light temperature and in-flight velocity of the melted material as a function of the stand-off distance between the torch head and the potential working plate surface.

The molten stream of particles should hit the surface of the working plate coupled to the ultrasonic power transducer. To determine the diameter of the plate, the distance at which the working plate should be mounted relative to the melting system is extremely important. It is affected primarily by the angle of convergence of the stream, the velocity of the particles in the stream, and the temperature of the particles over different distances, and has been validated to be between 100 mm and 300 mm (Figure 3). It was assumed that the diameter of the working plate should cover as much of the melted material stream as possible to improve the process efficiency. The working plate should at the same time maintain a high amplitude and uniform distribution of vibrations, so the homogeneous powders may be produced. Finally, the range of the considered diameters of the vibrating plate was 60 to 190 mm.

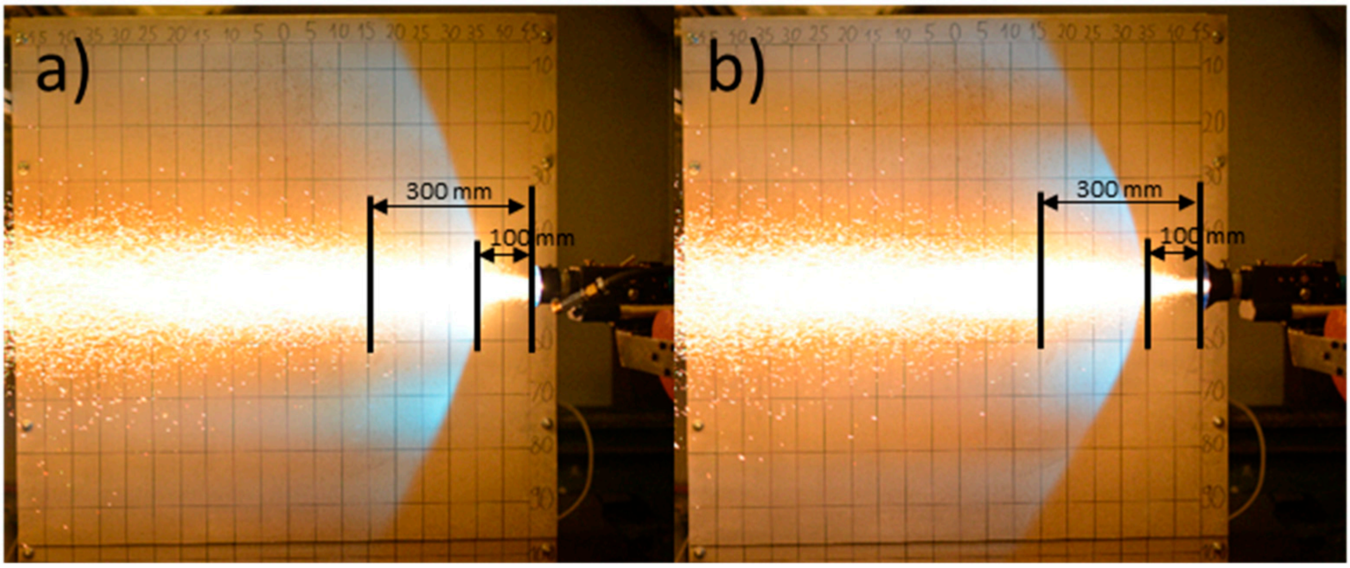

Figure 3. The view of the geometry of the arc melted metal stream: (**a**) lower (3 bars) and (**b**) higher (5 bars) working gas pressure.

3.2. Ultrasonic Waveguide Design Assumptions

The process of designing an ultrasonic tool (sonotrode) dedicated to the atomization of metals was carried out using the harmonic analysis with the finite element method (FEM). As the main design assumption, it was assumed that the basic self-vibration mode would be longitudinal vibrations of the sonotrode propagating as a transverse wave along the radius of the plate. The nominal frequency of the designed sonotrodes is 20 kHz and 70 kHz. The concepts of the two tool designs are presented below (Figure 4).

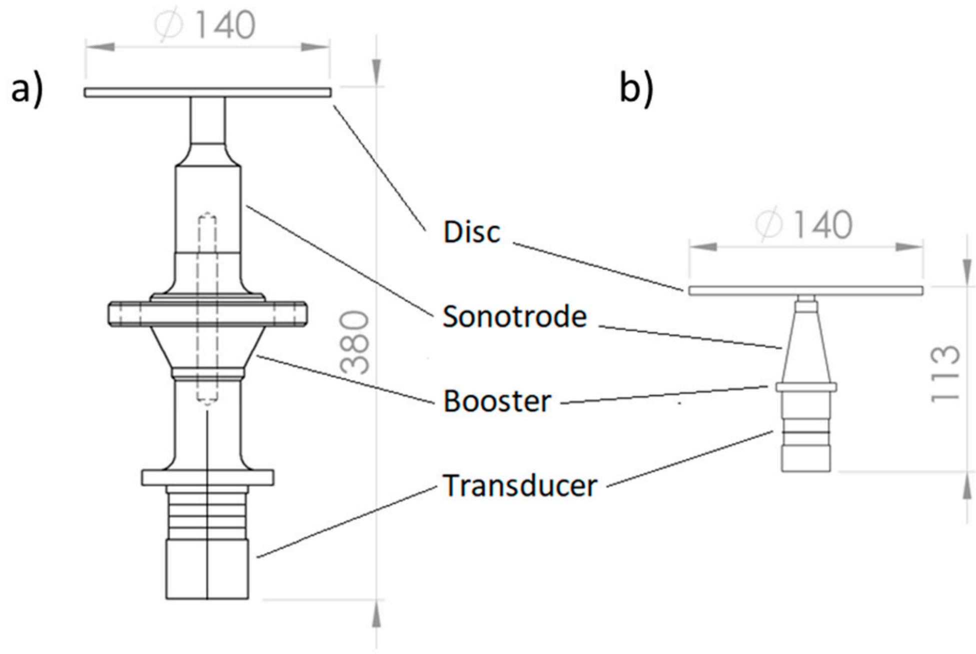

Figure 4. The concepts of the oscillating systems for atomization: (**a**) 20 kHz system, (**b**) 70 kHz system, all dimensions are given in mm.

4. Results and Discussion

4.1. Numerical Modelling

In the first design phase, both components (plate and sonotrode) were analyzed and optimized separately to obtain the appropriate vibration mode at the assumed resonant frequency of 20 kHz. This simplified the design process using a modal analysis. After obtaining satisfactory results, in the next step, the tool elements were assembled and the the entire sonotrode assembly was analyzed using a harmonic analysis. These studies allowed us to determine the predicted distribution of vibration amplitude on the working surface of the sonotrode and determine the area with the highest amplitude of vibrations. It was also possible to determine the maximum stresses that occur in the material during operation. The harmonic analysis was carried out under conditions of forced vibrations in the contact area within the following components of the waveguide.

Four models were analyzed, differing in the size of the working plate. The diameters of the plate were determined by the standing wavelength formed in the plate during resonance (~20 kHz). They were selected so that the smallest plate has one nodal point (with zero amplitude) and a diameter of 60 mm (Figure 5a). The larger plate, two-node one had a diameter of 108 mm (Figure 5b), the three-node plate had a diameter of 140 mm (Figure 5c) and the biggest, the four-node plate, had a diameter of 190 mm (Figure 5d). The calculations consisted of a modal analysis, necessary to design the appropriate geometry of the plate, and a harmonic analysis to determine the amplitudes of vibrations of the system. For all cases, the same sonotrode forcing (sinusoidal pressure with an amplitude of 50 MPa, which is the acceptable value for most types of materials) was used. In this way, it was possible to compare the effectiveness of the studied types of sonotrodes.

The vibration amplitudes at selected points of the plates are listed below:

- The maximum amplitudes of the single-node plate deflections in the deflection arrows, analyzed perpendicularly to the plate surface (57.3 μm, 44.5 μm)
- Maximum deflection amplitudes of a two-node plate in deflection arrows, analyzed perpendicularly to the plate surface (50.4 μm, 22.3 μm, 27.1 μm)
- Maximum deflection amplitudes of the three-node plate in the deflection, analyzed perpendicularly to the plate surface (36.9 μm, 32.5 μm, 22.0 μm, 27.7 μm)

- Maximum deflection amplitudes of the four-node plate in the deflection arrows, analyzed perpendicularly to the plate surface (32.1 μm, 26.3 μm, 19.2 μm, 14.7 μm, 17.3 μm)

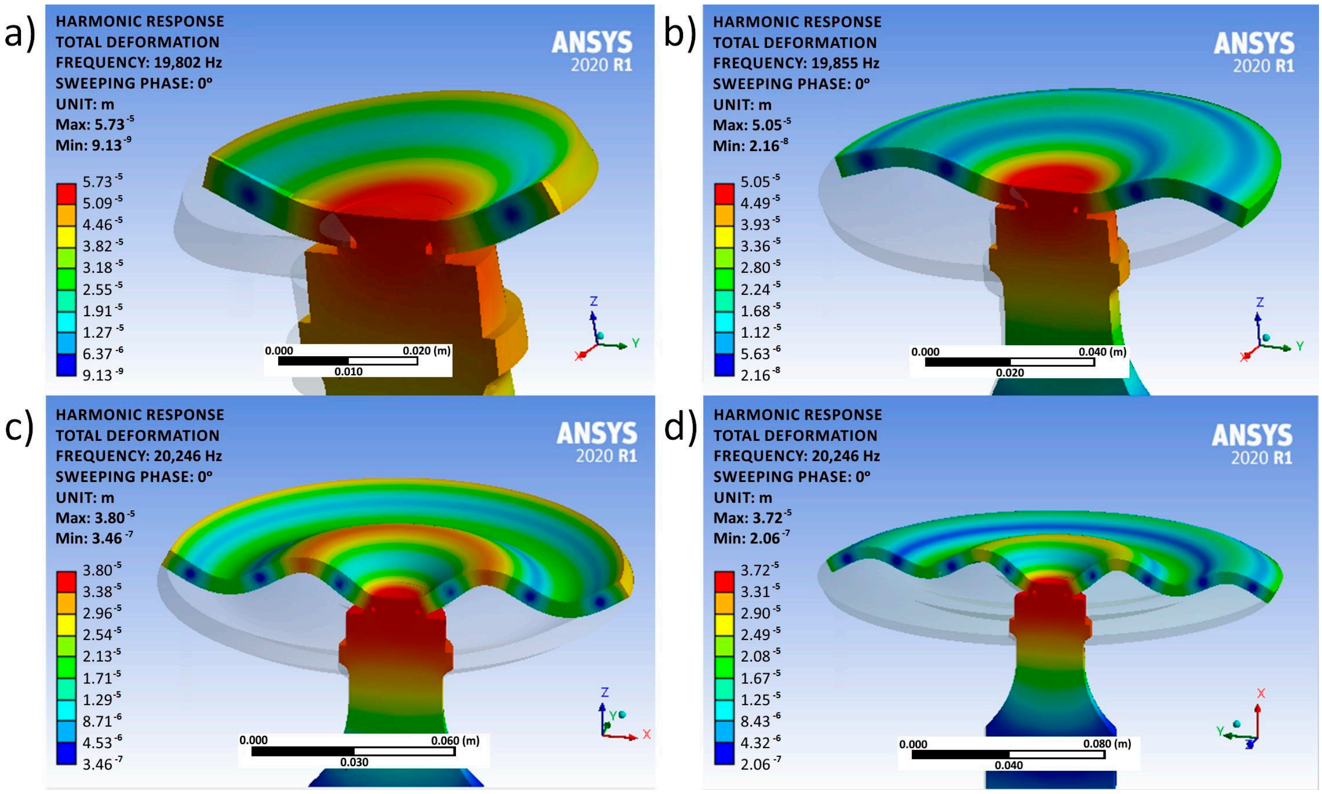

Figure 5. Sonotrode deformation at 20 kHz resonant frequency: (**a**) single-node, (**b**) two-node, (**c**) three-node and (**d**) four-node.

Due to the predicted diameter of the melted metal stream by the TWAS process (in the range of 80–130 mm for the pre-defined stand-off distances of 100 to 300 mm), the smallest plates, with diameters of 60 mm and 108 mm, seem to be insufficient. However, they provide the highest level of amplitude (in the central part of the plate >50 μm), which could have a significant impact on atomization efficiency. The sonotrode with a 190 mm working plate is sufficient for the assumed atomization conditions and the diameter of the melt stream, but it has the lowest amplitudes of the plate's deflections. Therefore, the selected solution here is a plate with a diameter of 140 mm. It meets both geometrical requirements, and provides a relatively high vibration amplitude of the plate surface.

Taking into account the above conclusions, the calculations for a sonotrode with a natural frequency of 70 kHz were carried out for one diameter only, of 140 mm. This was also intended choice, giving a possibility of comparing both systems in future, in terms of properties of the obtained powders.

The results of the calculation of the vibration distribution of the plate are shown below (Figure 6). As can be seen, a higher vibration frequency (70 kHz) results in more nodes and arrows of the deflection of the plate. This increases the probability of a metal particle hitting the vibrating area of the plate, which can positively affect the homogeneity of the resulting powders and the efficiency of the process.

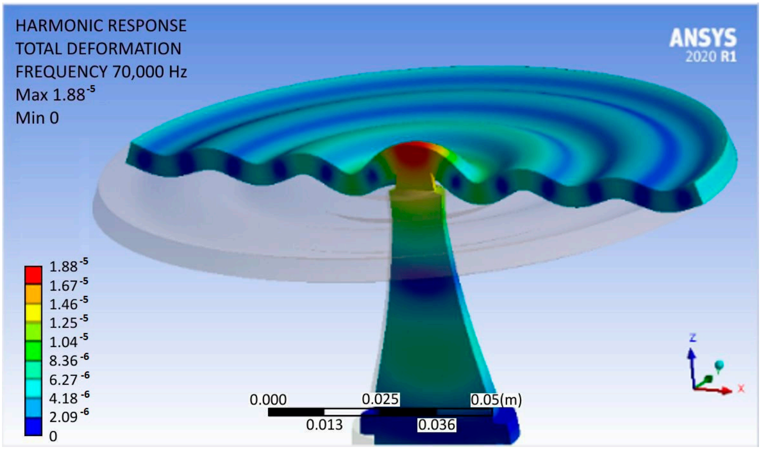

Figure 6. Distribution of vibration amplitudes with vibrations forced at a frequency of 70 kHz.

The presented forms of vibrations of the designed system confirm that it is properly tuned, and the distribution of vibrations on the surface of the plate is uniform around its entire circumference. The plate vibrates properly, without visible parasitic modes, which confirms that the elements of the oscillating system cooperate well with each other and do not introduce significant energy losses. The vibration amplitudes at selected points of the plate in the direction perpendicular to its surface are 18.1 µm; 7.7 µm; 6.0 µm; 5.0 µm; 5.5 µm; 3.5 µm; and 5.5 µm.

4.2. Working Plate Deflection Measurements

In order to verify the model and confirm the amplitude distribution on the surface of the sonotrode plate, measurements of the amplitude of vibrations on its surface were conducted. Due to the fact that sonotrodes are solids with rotational symmetry, the amplitude study was carried out at a series of points along the radius of the plate with a measuring step of 0.5 mm.

The ultrasonic transducers (20 kHz and 70 kHz) were tested together with mounted plates, each having a diameter of 140 mm. The ultrasonic waveguides were installed on a measuring table (Figure 7, as an example of 70 kHz set-up). The Keyence LK-H008 laser displacement sensor was directed at the surface of the sonotrode. It was moved along the plate by a precise micrometer screw.

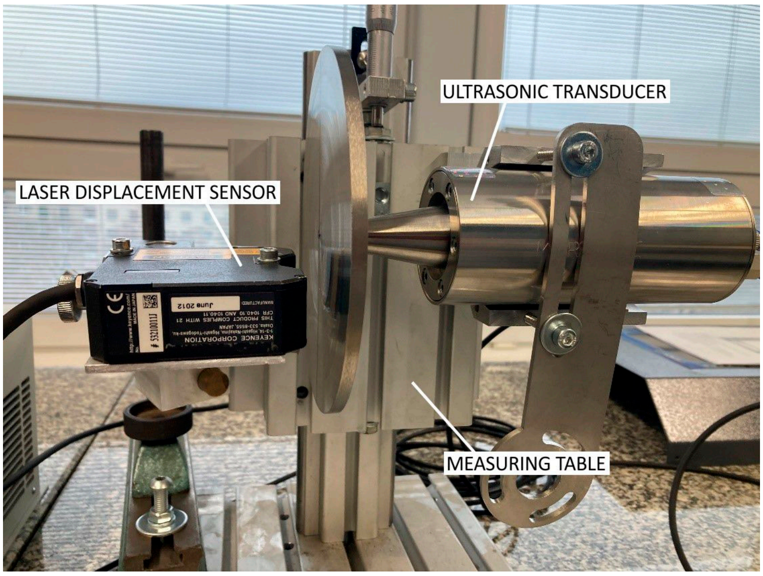

Figure 7. The measurement stand for testing the amplitude of the sonotrode vibrations.

Measurements were made cyclically by moving the optical sensor away from the axis of the sonotrode. At each point, the measurement was made four times by changing the generator amplitude setting. For the purpose of testing the 20 kHz system, amplitudes at four levels of 10%, 20%, 30% and 40% of the range were used, while for the 70 kHz system, 60%, 70%, 80% and 90% settings were used, whereas 100% of the energization corresponds to a maximum value of 1.8 kV supply voltage for a 20 kHz transducer and 300 V for a 70 kHz transducer. The obtained results are presented on a graph of the amplitude distribution depending on the distance from the center of the plate (Figure 8).

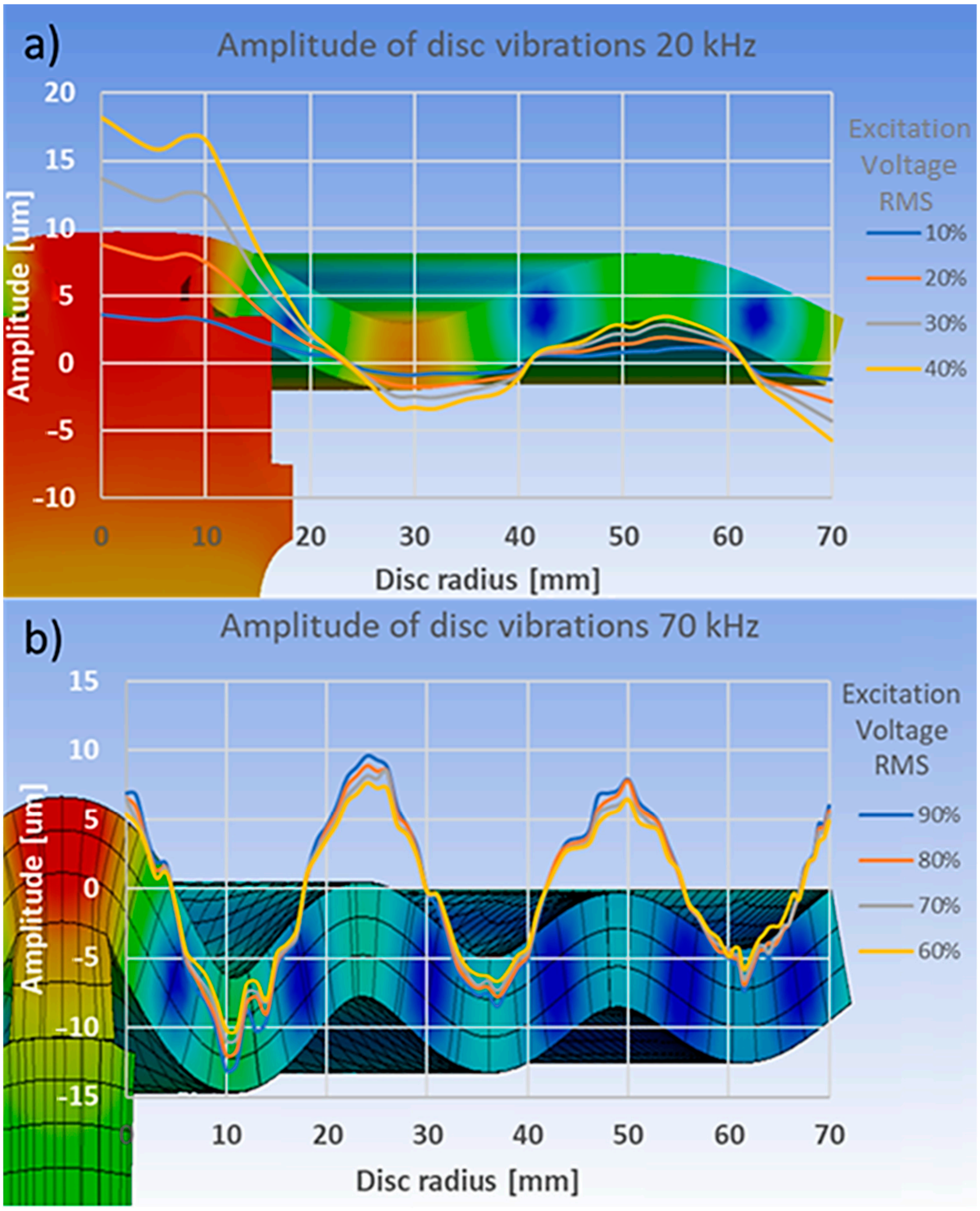

Figure 8. Amplitude distribution depending on the distance from the axis of the plate: (**a**) for the 20 kHz system and (**b**) for the 70 kHz system.

The results of numerical calculations and those obtained experimentally show a good correspondence. This mainly concerns the distribution of the amplitude of vibrations along the radius of the plate, in particular the position of the maxima and minima of the amplitude of the standing wave.

The amplitude values of the FEM model compared to those measured on the real object turned out to be lower. The differences result from the heterogeneity of material properties and the necessary approximations of the finite element method. In addition, the system was not powered by the maximum possible power (only 40% for the 20 kHz system) due to the lack of liquid load for atomization. A further increase in power without loading the system would risk damaging it. This does not change the fact that the study clearly confirmed the proper nature of vibrations of both sonotrodes, which was the most important goal of this experiment.

In addition, the results obtained from analytical calculations show that the amplitude of vibrations required to produce the atomization process is relatively small compared to the amplitude values obtained in the arrows (maxima) on the surface of the plate. Analyzing the vibration amplitude distribution for both vibration systems (20 kHz and 70 kHz), it can be seen that over 90% of the plate surface meets the theoretical amplitude condition, i.e., Am > 1.223 µm for 20 kHz and Am > 0.805 µm for 70 kHz for water (Table 1). For liquid metals, the required amplitudes have a mixed value, respectively, Am > 0.595 µm for 20 kHz and Am > 0.392 µm for 70 kHz, which confirms the suitability of both systems for atomization.

4.3. Observation of Ultrasonic Atomization of Water by High-Speed Camera

Verification of the operation of both ultrasonic systems was also made by the trials oriented at the atomization of distilled water on the surface of the sonotrode. The selection of water for the initial trials was done for two reasons: (i) ease and safety with its application; but also due to (ii) its lower acoustic impedance when compared to liquid metals. For this reason, if the atomization phenomenon can be effectively induced for water, the more probable that it will occur for liquid metals or metal alloys. The atomization processes were observed with the Phantom v12 high-speed camera. The frequency of registration of the atomization process of the droplet on the sonotrode plate was always higher than the frequency of vibrations of the plate: 22,000 fps for 20 kHz system and 72,000 fps for 70 kHz one. The images were recorded using a PC, connected via Ethernet interface and dedicated software (Phantom Camera Control 3.7). The test site of the atomization area was illuminated by a special reflector with a power of 5 kW. A dedicated image analysis tool allowed determining the time of individual stages of atomization and the particle size distribution of liquids after atomization for various process parameters. During the research, two vibration systems (20 kHz and 70 kHz) were used. For each, the power of the system was changed, and it was checked how the atomization proceeded at selected points on the plate. These points were selected on the basis of vibration amplitude measurements, and it was decided to investigate the phenomenon of droplet atomization both for arrows (amplitude maxima) and for nodes (amplitude minima). Below, the results of atomization tests recorded with a high-speed camera (Figure 9) are presented. The water droplet was placed in the center of the plate, and after 22 µs of its exposition to ultrasonic waves the phenomenon of cavitation occurs. After another 22 µs, fine droplets start to be released, while in 66 µs from when the UT system is switched on, the droplet completely explodes, which is accompanied by the phenomenon of the so-called ultrasonic fountain.

Figure 10 shows the individual frames obtained for the 70 kHz system. It can be clearly seen that the time from the moment of switching on the system to the moment of cavitation is twice as long. This is due to the characteristics of the 70 kHz system itself, which cannot be fine-tuned prior it is switched on. So, the delay is caused by tuning the system when turned on. However, from the moment of observing cavitation in a droplet of water (Figure 10b) to the time of triggering the phenomenon of the ultrasonic fountain (Figure 10d) about 44 µs have passed.

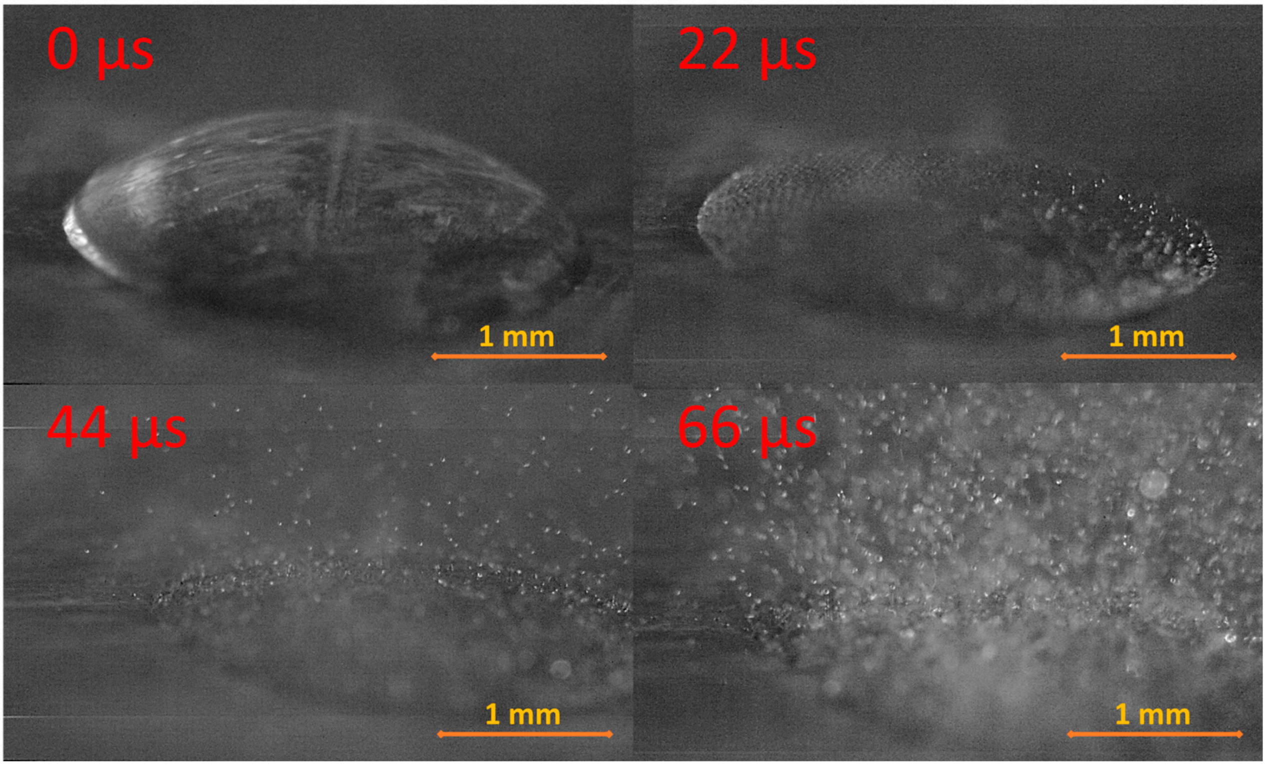

Figure 9. Atomization of a liquid droplet on the plate of a vibrating system with a resonant frequency of 20 kHz.

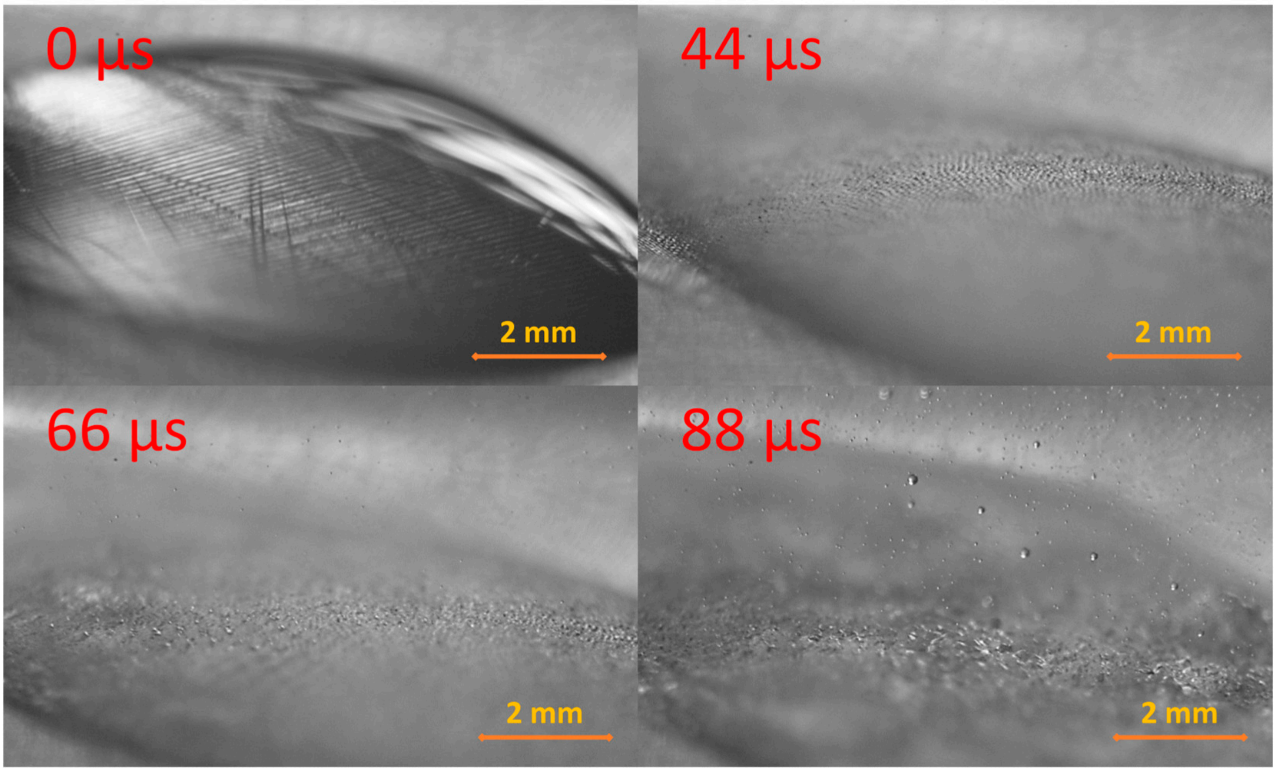

Figure 10. Atomization of a liquid droplet on a plate of the system with a resonant frequency of 70 kHz.

Selected photos of the process of atomization of water droplets on a macro scale are presented in Figure 11a,b and on the micro scale in Figure 11c,d. Macro photos show a fountain of liquid as a whole, and micro photos allow observing only selected fragments of a column of atomized droplets, but with a much higher resolution. They were recorded from a shorter distance, thanks to which it is possible to analyze the morphology of the droplets and make a histogram of the distribution of their size.

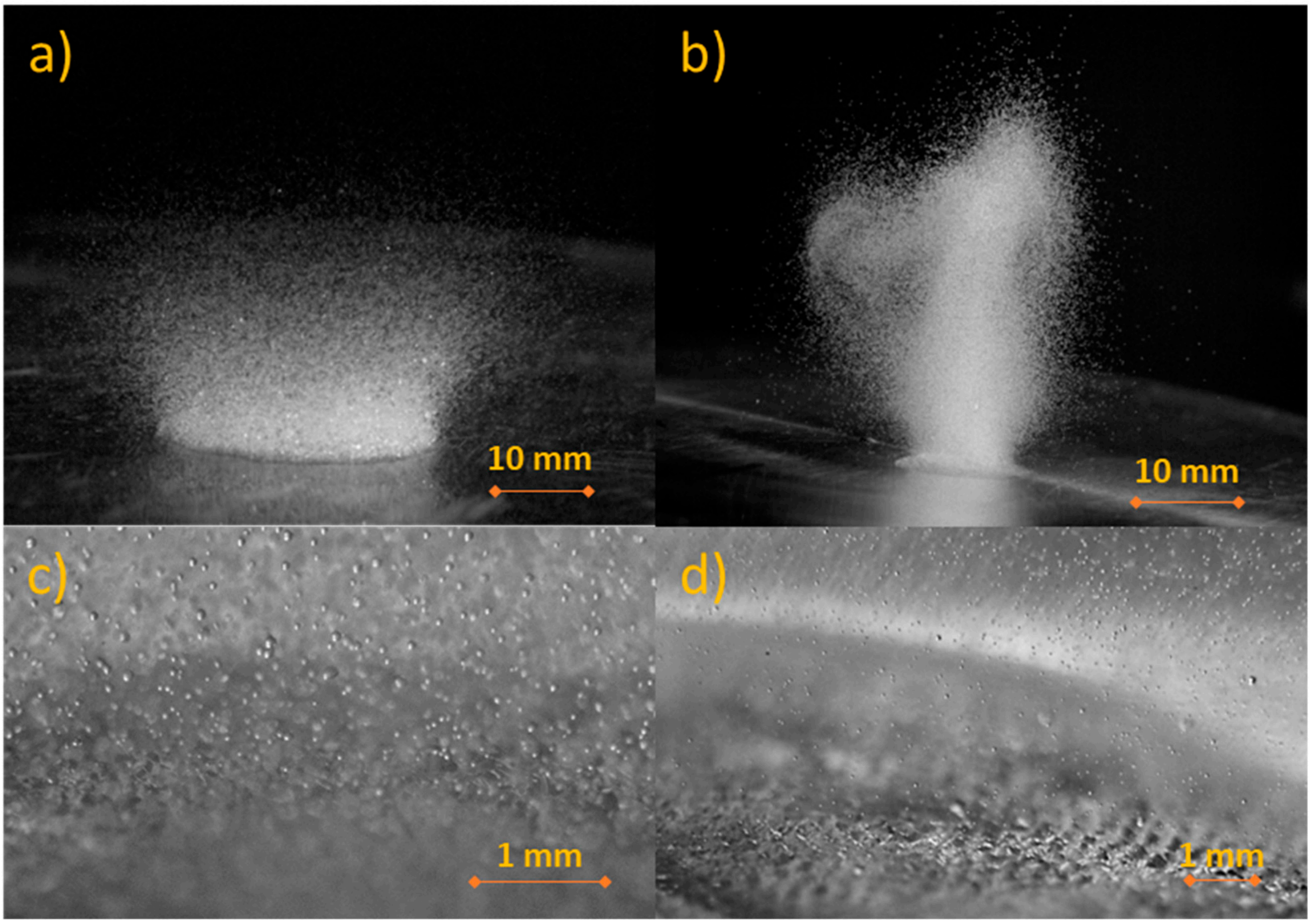

Figure 11. Droplet distribution for 20 kHz (**a**,**c**) and 70 kHz (**b**,**d**).

The analysis of images obtained from the high-speed camera was carried out in several key stages. In the first one, the single frames were selected for which the atomization process was stable, i.e., in the subsequent moments of registration, the particle size was comparable (Figure 12).

Then, it was necessary to extract the area of atomized particles from the image so that the external objects would not interfere with the post-analysis process. The areas representing the surface of the sonotrode and the liquid covering it, which has not yet been completely atomized, were removed (Figure 12d).

The next step was to adjust the background (Figure 13). For this purpose, a median filter was used to remove random peaks and a low-pass (averaging) filter was used to extract the background. This is achieved by using a filter mask the size of which (in pixels) exceeds the size of the largest droplet, which leads to the removal of droplets from the image and averaging the background. The background thus extracted was subtracted from the original image and the image was ready for the threshold process. The threshold value was chosen so that the image after binarization only took into account droplets without the background.

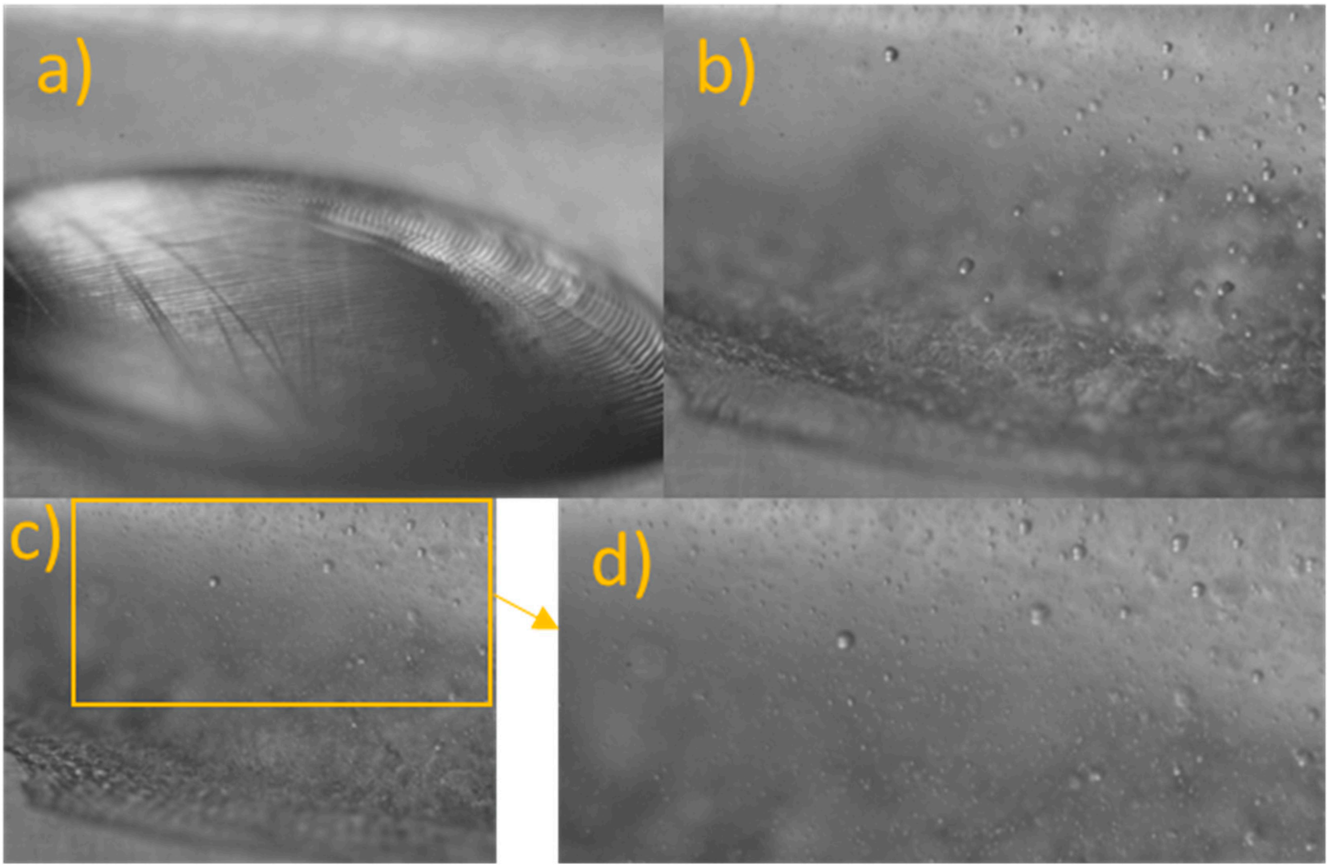

Figure 12. Selection of images for the analysis (**a**) 0 µs, (**b**) 80 µs, (**c**) 120 µs, (**d**) extracted fragment.

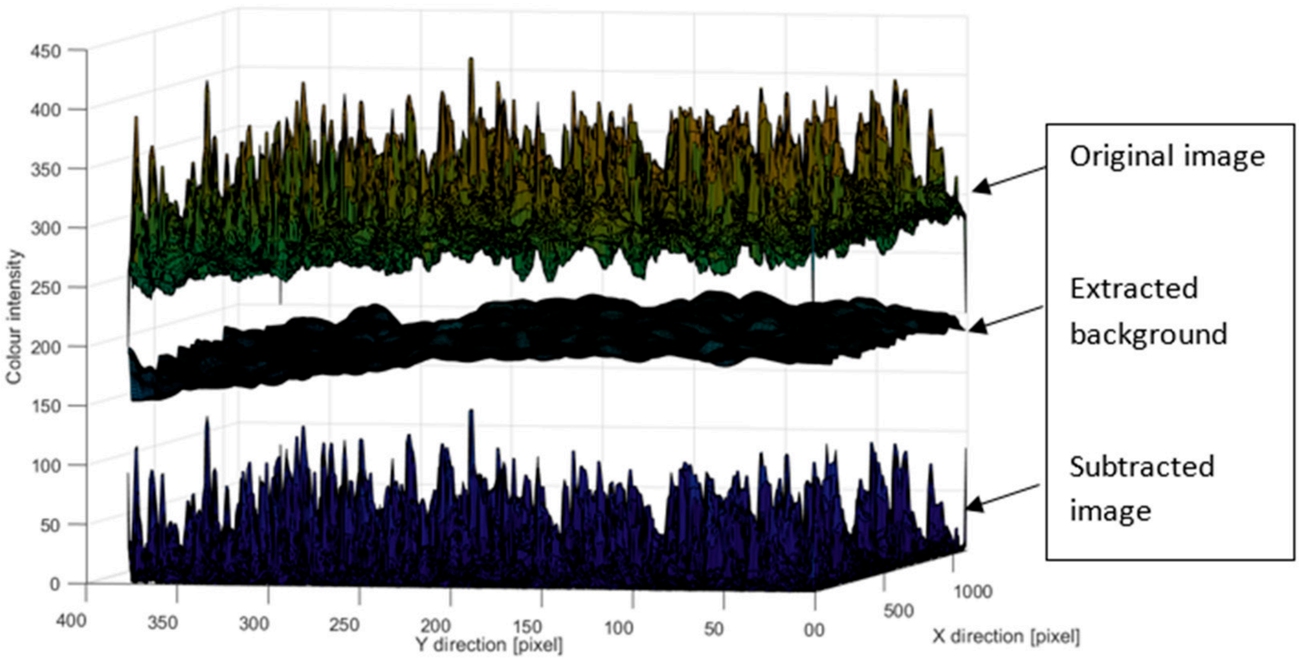

Figure 13. Image background extraction and alignment.

After image binarization, the "regionprops" function of the Matlab image pressing package was used. This function returns the results of measurements of objects in a black and white binary image. It allows determining the x and y coordinates of the detected regions and their equivalent diameter. This function finds unique objects in a binary image using 8-connected 'neighboring' regions of pixels (oriented horizontally, vertically or diagonally) for 2-D images. So, the pixels are considered as a part of the same object if their edges or corners are connected. The exemplary results for 70 kHz ultrasonic atomization set-up are shown in Figure 14.

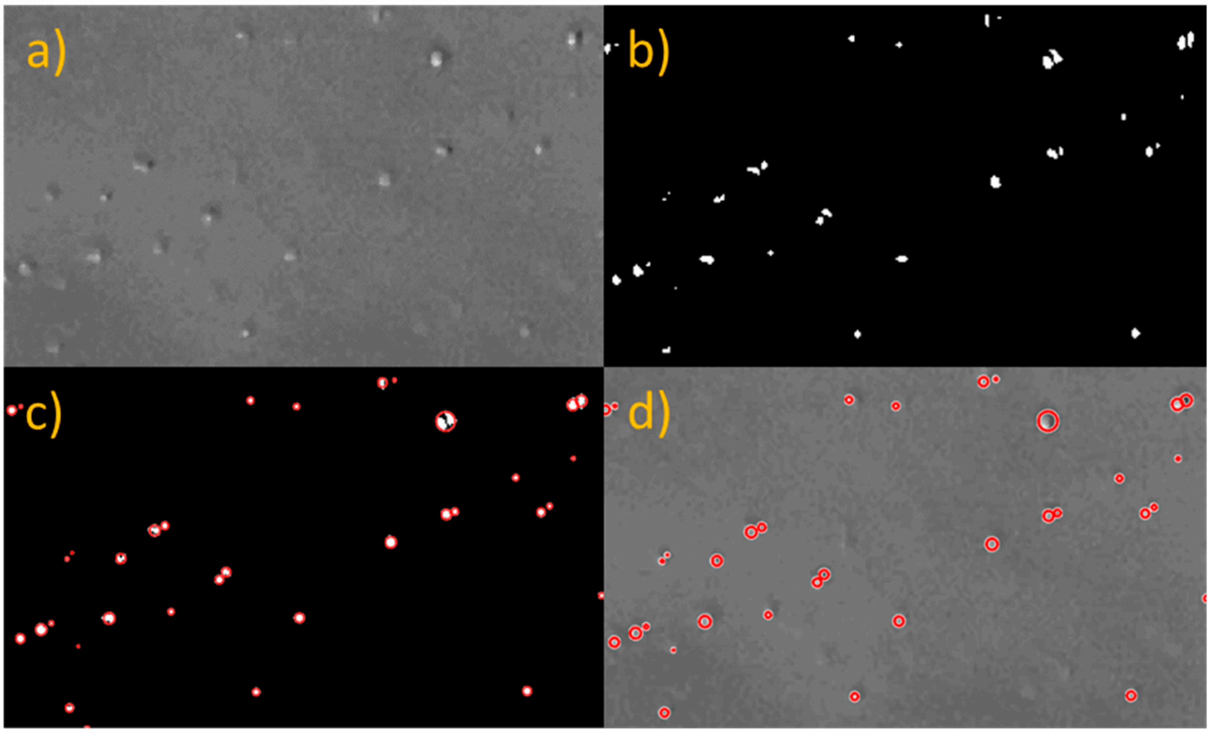

Figure 14. Droplets detection: (**a**) gray scale image, (**b**) image after binarization, (**c**) image with recognized regions (marked with the red circles) and (**d**) verification of the image processing.

In the next step, the droplet size distribution results were obtained and compared. A histogram showing the comparison of results obtained for 20 kHz and 70 kHz transducers is presented in Figure 15.

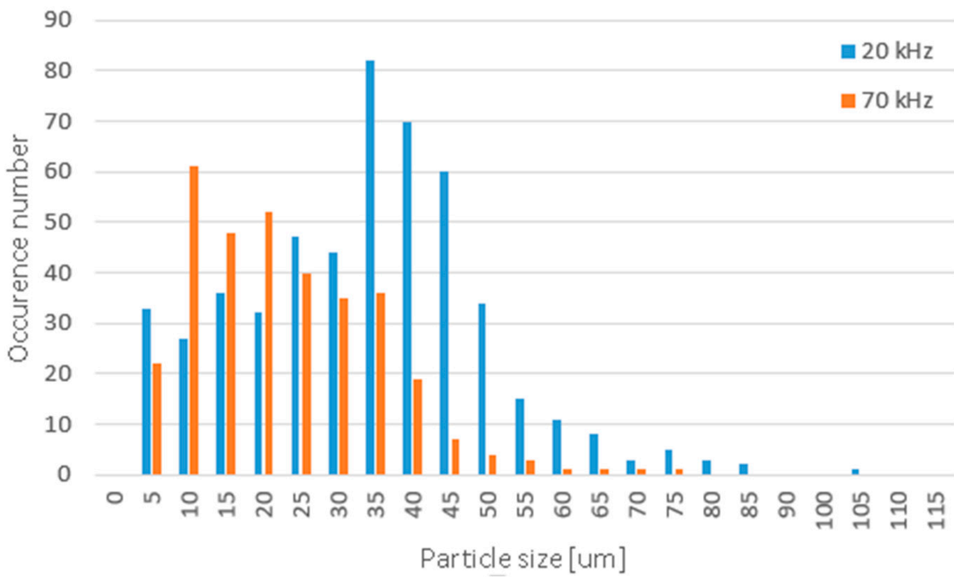

Figure 15. Comparison of droplet size distribution for 20 kHz and 70 kHz.

It can be clearly seen that for a 20 kHz transducer, particles of 35 μm dominate, and at least 50% of the produced particles are in the range of 35–55 μm. It should be noted that this result corresponds to the average droplet size calculated analytically (2), i.e., 55 μm. In the case of a 70 kHz transducer, a clear decrease in particle size can be seen. The size of 10 μm dominates, and at least 50% of the particles are in the range of 10–25 μm. The analytically calculated size is 24 μm for 70 kHz transducer frequency. Moreover, the results obtained experimentally for both 20 kHz and 70 kHz systems correspond well to the results that can be found in the literature, as calculated in a range of 20 to 100 kHz by Sarkovic and Babovic [22], numerically analyzed in a range of 50 to 200 kHz by Sugondo et al. [23] or experimentally tested for 35 kHz ultrasonic system by Panao [24]. In turn, the analytically calculated values for liquid metal are 86 μm for 20 kHz and 37 μm for 70 kHz, respectively. The obtained results allow concluding that for liquid metals, the size of the obtained particles will be about 30–40% higher than for water, for both considered oscillating systems; that would be a very positive desired outcome. The current interest in metal powders and metal alloys, due to the characteristics of modern manufacturing technologies, mainly concerns materials in the range of 10–100 μm [25,26].

5. Conclusions

The article presents an analysis of the operation of two ultrasonic systems with different operating frequencies (20 kHz and 70 kHz). All stages of the design of these systems (FEM calculations, harmonic analysis and obtained forms of vibrations) are presented in this work. After the manufacturing of both ultrasonic systems, the results of sonotrode deflection measurements are presented. This allowed us to verify and confirm the correctness of the designing process and construction. By comparing the expected amplitude distribution in the numerical model to the experimental results, it can be concluded that the assumptions to the model, as well as the calculation process, was correct.

The functional tests of both devices were carried out for different operating parameters (amplitude of voltage powering the sonotrode). The atomization process of the distilled water was recorded with a high-speed camera, which allowed us to confirm that the frequency of the transducer significantly affects the size of the atomized droplets. However, both systems proved to be highly effective in terms of atomization. In addition, it can be noted that:

- FEM simulation results and experimental measurements show a very similar distribution of vibration amplitude, especially when comparing the range of maxima and minima of the standing wave for both working plates.
- The calculated minimum vibration amplitude thresholds required to initiate the atomization process were reached for both developed ultrasonic atomization systems for more than 90% of the surface, in both set-ups (20 kHz and 70 kHz).
- The size of the atomized water droplets during the tests indicates that the 20 kHz system generates droplets in the range of 10–25 μm and the 70 kHz system in the range of 35–55 μm.
- The obtained results of the morphological analysis are in agreement with the results of the analytical calculations. The lower droplet diameters were obtained for individual systems experimentally when compared to those calculated analytically. However, the mutual trend is maintained, i.e., for a system with a higher frequency, the droplets have on average an over 50% smaller diameter.

The obtained results confirm the effectiveness of the developed atomization system for water, and according to the calculations, the systems should allow production of metal powder particles with a desired size distribution. In further research, the developed ultrasonic atomization systems will be loaded with a stream of molten metal droplets to see if the atomization can be still effectively performed.

Author Contributions: Conceptualization, P.K. (Pawel Kustron), M.K. and P.S.; methodology, P.K. (Pawel Kustron), M.K., A.S. and P.S.; investigation, P.K. (Pawel Kustron), M.K., A.S., T.P., P.K. (Pawel Kaczynski) and P.S.; writing—original draft preparation, P.K. (Pawel Kustron), M.K., A.S. and P.S.; and writing—review and editing, P.K. (Pawel Kustron), M.K., A.S., T.P. and P.S. All authors have read and agreed to the published version of the manuscript.

Funding: This research was funded by the National Center for Research and Development in Poland, under the LIDER program (LIDER/42/0230/L-10/18/NCBR/2019).

Institutional Review Board Statement: Not applicable.

Informed Consent Statement: Not applicable.

Data Availability Statement: The data generated and/or analyzed during the presented study are available from the corresponding author upon request.

Acknowledgments: The authors would like to acknowledge the financial support provided by the National Center for Research and Development in Poland, under the LIDER program (LIDER/42/0230/L-10/18/NCBR/2019) awarded to the Faculty of Mechanical Engineering at Wroclaw University of Science and Technology.

Conflicts of Interest: The authors declare no conflict of interest.

References

1. Dobre, M.; Bolle, L. Visualisation and Analysis of Liquid Film Surface Patterns Formed on Ultrasonic Atomisers. In Proceedings of the ILASS-Europe 1999, Toulouse, France, 15–17 July 1999.
2. Naidu, H.; Kahraman, O.; Feng, H. Novel Applications of Ultrasonic Atomization in the Manufacturing of Fine Chemicals, Pharmaceuticals, and Medical Devices. *Ultrason. Sonochemistry* **2022**, *86*, 105984. [CrossRef] [PubMed]
3. Qu, S.; Zhang, C.; Liang, Y.; Ma, Z.; Meng, F.; Wang, Z.; Xu, P.; Yu, T.; Zhao, J. Experimental Investigation of Ultrasonic-Vibration Polishing of K9 Optical Glass Based on Ultrasonic Atomization. *Ceram. Int.* **2022**, *48*, 9067–9074. [CrossRef]
4. Galleguillos, R. Acoustic Cavitation Detection during Ultrasonic Atomization Process. *Appl. Acoust.* **2022**, *192*, 108716. [CrossRef]
5. Guerra-Bravo, E.; Lee, H.-J.; Baltazar, A.; Loh, K.J. Vibration Analysis of a Piezoelectric Ultrasonic Atomizer to Control Atomization Rate. *Appl. Sci.* **2021**, *11*, 8350. [CrossRef]
6. Ramisetty, K.A.; Pandit, A.B.; Gogate, P.R. Investigations into Ultrasound Induced Atomization. *Ultrason. Sonochemistry* **2013**, *20*, 254–264. [CrossRef] [PubMed]
7. Jedynak, A.; Ertugrul, G.; Neumann, A.; Pippig, R.; Härtel, S. Semi-Finished Powder of Aluminum Matrix Composite for a Direct Energy Deposition Additive Manufacturing. *Mater. Res. Proceeding* **2023**, *28*, 199–206.
8. Żrodowski, Ł.; Wróblewski, R.; Choma, T.; Morończyk, B.; Ostrysz, M.; Leonowicz, M.; Łacisz, W.; Błyskun, P.; Wróbel, J.S.; Cieślak, G.; et al. Novel Cold Crucible Ultrasonic Atomization Powder Production Method for 3D Printing. *Materials* **2021**, *14*, 2541. [CrossRef]
9. Hinrichs, F.; Kauffmann, A.; Schliephake, D.; Seils, S.; Obert, S.; Ratschbacher, K.; Allen, M.; Pundt, A.; Heilmaier, M. Flexible Powder Production for Additive Manufacturing of Refractory Metal-Based Alloys. *Metals* **2021**, *11*, 1723. [CrossRef]
10. Grzelak, K.; Bielecki, M.; Kluczyński, J.; Szachogłuchowicz, I.; Śnieżek, L.; Torzewski, J.; Łuszczek, J.; Słoboda, Ł.; Wachowski, M.; Komorek, Z.; et al. A Comparative Study on Laser Powder Bed Fusion of Differently Atomized 316L Stainless Steel. *Materials* **2022**, *15*, 4938. [CrossRef]
11. Alavi, S.H.; Harimkar, S.P. Ultrasonic Vibration-Assisted Laser Atomization of Stainless Steel. *Powder Technol.* **2017**, *321*, 89–93. [CrossRef]
12. Monti, C.; Turani, M.; Papis, K.; Bambach, M. A New Al-Cu Alloy for LPBF Developed via Ultrasonic Atomization. *Mater. Des.* **2023**, *229*, 111907. [CrossRef]
13. Sheng, L.Y.; Zhao, H. Investigation of Al-Si-Cu-Zn-Y-Base Alloy Powders Prepared by Ultrasonic Gas Atomization for Brazing of an Al-Base Alloy. *Strength Mater.* **2021**, *53*, 591–600. [CrossRef]
14. Shu, Q.Q.; Shi, J.T.; Liu, J.; Deng, Z.S. Ultrasonic Preparation of Submicron Low Melting Point Alloy Powder. *Mater. Sci. Forum* **2020**, *993*, 333–343. [CrossRef]
15. Cheeke, J.D.N. *Fundamentals and Applications of Ultrasonic Waves*; CRC Series in Pure and Applied Physics; CRC Press: Boca Raton, FL, USA, 2002; ISBN 978-0-8493-0130-8.
16. Lierke, E.G.; Grießhammer, G. The Formation of Metal Powders by Ultrasonic Atomization of Molten Metals. *Ultrasonics* **1967**, *5*, 224–228. [CrossRef]
17. Rajan, R.; Pandit, A.B. Correlations to Predict Droplet Size in Ultrasonic Atomisation. *Ultrasonics* **2001**, *39*, 235–255. [CrossRef]
18. Sheikhaliev, S.M.; Popel', S.I. Production of Metal Powders by Ultrasonic Atomization of Melts. *Sov. Powder Metall. Met. Ceram.* **1983**, *22*, 793–798. [CrossRef]
19. Wisutmethangoon, S.; Plookphol, T.; Sungkhaphaitoon, P. Production of SAC305 Powder by Ultrasonic Atomization. *Powder Technol.* **2011**, *209*, 105–111. [CrossRef]

20. Briceño-Gutierrez, D.; Salinas-Barrera, V.; Vargas-Hernández, Y.; Gaete-Garretón, L.; Zanelli-Iglesias, C. On the Ultrasonic Atomization of Liquids. *Phys. Procedia* **2015**, *63*, 37–41. [CrossRef]
21. Assael, M.J.; Kakosimos, K.; Banish, R.M.; Brillo, J.; Egry, I.; Brooks, R.; Quested, P.N.; Mills, K.C.; Nagashima, A.; Sato, Y.; et al. Reference Data for the Density and Viscosity of Liquid Aluminum and Liquid Iron. *J. Phys. Chem. Ref. Data* **2006**, *35*, 285–300. [CrossRef]
22. Šarkovic, D.; Babovic, V. On The Statistics Of Ultrasonically Produced Water Droplets. *Z. Naturforschung A* **2005**, *60*, 489–493. [CrossRef]
23. Sugondo, A.; Sutrisno; Anggono, W.; Anne, O. Effect of Frequency on Droplet Characteristics in Ultrasonic Atomization Process. *E3S Web Conf.* **2019**, *130*, 01002. [CrossRef]
24. Panão, M. Ultrasonic Atomization: New Spray Characterization Approaches. *Fluids* **2022**, *7*, 29. [CrossRef]
25. Shishkovsky, I. *New Trends in 3D Printing*; BoD—Books on Demand: Norderstedt, Germany, 2016; ISBN 978-953-51-2479-5.
26. Averardi, A.; Cola, C.; Zeltmann, S.E.; Gupta, N. Effect of Particle Size Distribution on the Packing of Powder Beds: A Critical Discussion Relevant to Additive Manufacturing. *Mater. Today Commun.* **2020**, *24*, 100964. [CrossRef]